

Magnetic properties and electronic structures of $(\text{YTiO}_3)_2/(\text{BaTiO}_3)_n$ superlattices

P. X. Zhou,^{1,3} H. M. Liu,¹ Z. B. Yan,¹ S. Dong,^{2,a)} and J.-M. Liu^{1,a)}

¹Laboratory of Solid State Microstructures, Nanjing University, Nanjing 210093, China

²Department of Physics, Southeast University, Nanjing 211189, China

³School of Science, Nantong University, Nanjing 226007, China

(Presented 7 November 2013; received 21 September 2013; accepted 30 October 2013; published online 6 February 2014)

The magnetic properties and electronic structures of $(\text{YTiO}_3)_2/(\text{BaTiO}_3)_n$ superlattices are investigated using the first-principles calculations. It is revealed that the in-plane compressive strain results in the A-type antiferromagnetic order in the YTiO_3 component. Surprisingly, the Ti ions in BaTiO_3 layers exhibit a weak ferromagnetic order for $n=4$. The ferromagnetism in the BaTiO_3 layers near the interface is related to the polar discontinuity of YTiO_3 and ferroelectric polarization of BaTiO_3 . The electronic structures indicate that the $n=4$ superlattice shows the two-dimensional electron gas at the interface. © 2014 AIP Publishing LLC. [<http://dx.doi.org/10.1063/1.4863489>]

Oxide superlattices and heterostructures have received attention due to the abundant interfacial effects and diverse physical properties. Typical examples include the two-dimensional electron gas (2DEG), interfacial superconductivity, improper ferroelectricity, and charge order in various oxide heterostructures and superlattices.^{1–6} Those superlattices and heterostructures, consisting of one component with electro-polar termination and the other with electro-neutral termination, have attracted plenty of interest in experiments⁷ and theories.^{8–12} The observed and predicted effects seem to be very materials-dependent, but the polar-termination or discontinuity becomes a key ingredient for these fascinating phenomena.^{13–15}

The perovskite rare-earth titanate $RTiO_3$ family exhibits rich physics involving orbital, magnetic, and transport behaviors.^{16–18} Although the whole $RTiO_3$ family shares the same crystal space group, the magnetic ground states depend on the size of R ions. The Ti^{3+} spins favor the G-type antiferromagnetic (G-AFM) order when R ion is relatively large (e.g., from La to Sm), but the ferromagnetic (FM) order is preferred when R ion is small (e.g., from Gd to Yb, and Y).^{19–21} The spin order of Ti ions is sensitive not only to the size of R ion, but also to the strain. YTiO_3 (YTO) is FM in bulk form but is predicted to exhibit the A-type antiferromagnetic (A-AFM) order in thin film form epitaxially grown on the (001) LaAlO_3 (LAO) substrate.²²

In contrast, the ATiO_3 (A: divalent alkaline earths) family with Ti^{4+} cation shows quite different physical properties. BaTiO_3 (BTO) is a traditional ferroelectric (FE) without magnetic. These differences between $RTiO_3$ and ATiO_3 suggest that the A site ionic size, B-site ionic valence, external stimuli, and various combinations of the members in the two families can be efficient approaches to invent novel properties or modulate existing ones with sufficient degrees of freedom.

In this work, the magnetic ground states and electronic structures of $(\text{YTiO}_3)_2/(\text{BaTiO}_3)_n$ (YTO/BTO) superlattices,

which are assumed to grow epitaxially on (001) SrTiO_3 substrates, are investigated by means of the first-principles calculations. Here, the subscripts 2 and n denote the unit layer numbers of YTO and BTO, respectively. Three interesting physical issues can be expected. First, YTO/BTO interface has polar discontinuity due to the valence difference between Y^{3+} and Ba^{2+} (Ti^{3+} and Ti^{4+}), probably inducing novel interfacial effects and even electron redistribution over not only the interfacial regime. Second, BTO is a typical ferroelectric, allowing a degree of freedom to modulate the interfacial electrons by FE polarization. Third, the magnetic order of YTO is sensitive to strain and may be also tuned by the interfacial electrons. Therefore, the spontaneous symmetry breaking and geometrical confinement within these ultrathin superlattices will enforce electronic reconstruction in both YTO and BTO.

The space group of bulk YTO is $Pbnm$ and the lattice constants are $a = 5.358 \text{ \AA}$, $b = 5.696 \text{ \AA}$, and $c = 7.637 \text{ \AA}$. The space group of bulk BTO is $P4mm$ and the lattice constants are $a = b = 3.995 \times \sqrt{2} = 5.648 \text{ \AA}$, $c = 4.034 \text{ \AA}$. STO is adopted as the substrate with a cubic lattice $a = b = c = 3.905 \text{ \AA}$. The in-plane lattice constants of YTO and BTO are fixed to match STO: $a_0 = b_0 = 3.905 \times \sqrt{2} = 5.523 \text{ \AA}$. The biaxial average compressive strains of YTO and BTO on STO substrate, as estimated from $[ab/a_0b_0]^{1/2} - 1$, are about 0.04% and 2.29%, respectively. The tiny lattice mismatch makes a synthesis of the YTO/BTO superlattices promising experimentally.

Our first-principles calculations are performed using the VASP (Vienna *ab-initio* simulation package) code^{23,24} within the generalized gradient approximation GGA + U method with the Perdew-Becke-Erzenhof function.²⁵ In the following calculations, the Hubbard U is imposed on Ti d states, and the Dudarev method²⁶ is implemented with $U_{\text{eff}} = 3.2 \text{ eV}$.²⁷ The plane-wave energy cutoff is 500 eV, and the Hellman-Feynman forces are 0.01 eV/Å during the optimization. In this work, two situations $n=2$ and $n=4$ BTO layers are studied as the representative cases.

It should be mentioned that conventional density functional theory may induce a pathological charge transfer from

^{a)}Authors to whom correspondence should be addressed. Electronic addresses: sdong@seu.edu.cn and liujm@nju.edu.cn

metal to ferroelectric due to the well-known drawback of band gap underestimation for insulators. This effect may be important in many cases.^{11,12} In the present case, YTO itself is not a metal but a Mott insulator. Both YTO and BTO are Ti-oxides (Ti^{3+} vs Ti^{4+}), in analogy to previous studied LaMnO_3 - SrMnO_3 superlattices, where LaMnO_3 is a Mott insulator while SrMnO_3 is a band insulator.⁸ In these cases, the identical ions guarantee the band-alignment issue automatically, and thus the physical mechanism discussed here may not be affected in the qualitative sense.

First, the magnetic order and electronic structure of bulk YTO are calculated. To obtain the magnetic ground state, the total energies of A-type, C-type, and G-type AFM states and FM state are calculated. It is found that the FM state is the magnetic ground state and the average magnetic moment of Ti ions is $0.885 \mu_B$, which is in agreement with earlier calculations²² and very close to experimental results.²⁸ The total density of states (DOS) of bulk YTO is shown in Fig. 1(a), indicating that YTO is an insulator with an energy gap of 1.56 eV, slightly larger than experimental value (~ 1.2 eV).²⁹

To study the strain effect alone, the magnetic ground state and electronic structure of YTO layer on STO substrate are investigated. Similar to the situation on LAO substrate,²² YTO is subjected to compressive strain and does display the A-type AFM. The physical reason may be due to the anisotropic strains that are individually significant along the a -axis (-2.98%) and b -axis (3.14%). The total DOS is displayed in Fig. 1(b), and YTO retains insulator with an energy gap of ~ 1.53 eV. Thus, the strain effect only changes the magnetic order of YTO, but does not change the insulation.

The magnetic and electronic structures of $(\text{YTO})_2/(\text{BTO})_n$ ($n=2$ and 4) superlattices on STO substrate are studied. The schematic structures of the two superlattices are illustrated in Figs. 2(a) and 3(a), respectively. First of all, the in-plane lattice constants of BTO are fixed to those of STO, then the lattice constant along the c axis and the atomic positions are optimized. After that, the optimized YTO and BTO on STO substrate are connected together to build the superlattices. Finally, the lattice length along the c axis (c_{SL}) and the atomic positions are fully optimized. The optimized c_{SL} are 16.37 Å and 25.32 Å for $(\text{YTO})_2/(\text{BTO})_2$ and $(\text{YTO})_2/(\text{BTO})_4$, respectively. After obtaining the values of

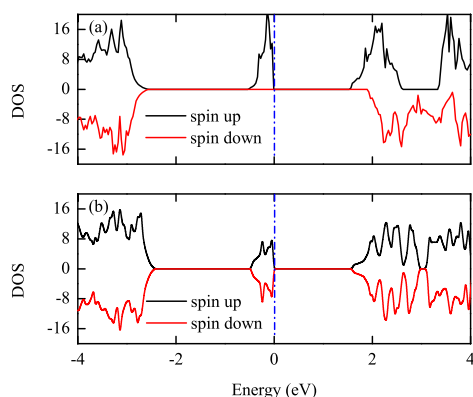


FIG. 1. Calculated spin-resolved DOS of YTO. (a) Bulk YTO and (b) YTO film on STO substrate. The Fermi energy is positioned as zero.

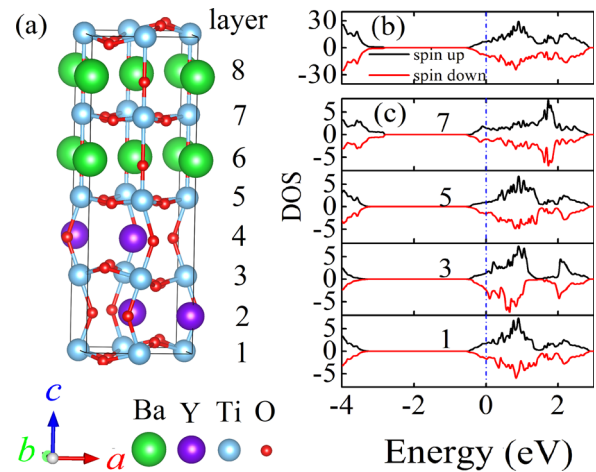


FIG. 2. (a) Schematic crystal structure of $(\text{YTO})_2/(\text{BTO})_2$. (b) Calculated spin-resolved total DOS, and (c) calculated PDOS of $(\text{YTO})_2/(\text{BTO})_2$. The Fermi energy is positioned as zero.

c_{SL} , various magnetic orders of the YTO component are imposed and all the atomic positions are further relaxed.

For the $n=2$ case, the BTO layer is too thin to retain its ferroelectricity. The total DOS and layer-projected DOS (PDOS) calculations show the whole metallicity across the superlattice, as exhibited in Figs. 2(b) and 2(c). Considering the insulating YTO and BTO, the metal state (conduction charge) is believed to originate from the interface charge reconstruction due to two competitive effects.¹⁰ The electrostatic potential in this superlattice is to constrain the charge to the interface, while the quantum kinetic energy is to make the t_{2g} electron to spread over all Ti ions. The electrostatic potential is the superposition of the polar discontinuous potential from the YTO and the FE potential from the BTO. Since the ferroelectricity in BTO is almost completely suppressed, the effect from the potential is relatively weak, insufficient to constrain the interfacial charge and thus the quantum kinetic energy makes the superlattice metallic. The total magnetic moment of the lattice is $\sim 0.08 \mu_B$. The moment quenching in this ultra-thin superlattice is due to the charge transfer from the YTO to the BTO. The projected electron densities over the d orbitals of the eight Ti ions are 0.4177, 0.4177, 0.4184, 0.4100, 0.3379, 0.3387, 0.4241, and 0.4226 in unit of electron charge. These values are obtained within the Wigner-Seitz spheres as specified by VASP, which are not very accurate but still qualitatively preferable. This distribution of electron densities, with a weak charge disproportionation smaller than 0.10, can be considered to be nearly uniform. The fractional $3d$ electron on each Ti is disadvantageous to form a Mott insulator.

Different from the $n=2$ thin case, for the thick $n=4$ case, our calculations reveal a quite novel magnetic profile. A significantly large magnetic moment up to $\sim 1.78 \mu_B$ emerges mainly from the BTO layer, while the YTO layer remains the AFM order. This ferromagnetism can also be observed from the total DOS and PDOS (Figs. 3(b) and 3(c)). The states at the Fermi level are mainly contributed by the 11th atomic layer (the interfacial layer in the BTO), implying the interfacial 2DEG. This is another example in

which the interfacial 2DEG and ferromagnetism coexist, an interesting result with some additional physics.

According to previous studies on LAO/STO, the interfacial 2DEG originates from the polar discontinuity and electrostatic doping of the STO layer.^{10,11} However, in the current study, the 2DEG is nontrivially different from the LAO/STO case, since our PDOS shows asymmetric behaviors. For example, the 7th atomic layer shows a quite different PDOS, without the 2DEG, although it seems to be a mirror of the 11th atomic layer. The asymmetry can be also evidenced between the 1st and 5th atomic layers. This anomalous asymmetry is due to the residual FE polarization of BTO layer pointing from the 5th atomic layer to the 11th atomic layer, which breaks the space inversion symmetry.

To qualitatively understand the results in the $n=4$ case, the electron potentials from both the FE polarization and polar interfaces are sketched in Fig. 4. If no polarization in the BTO layer is assumed ($P=0$), the electrostatic potential profile from the $(YO)^+$ atomic layers and thus the electron density should be symmetric, as shown in Fig. 4(b). A nonzero polarization (P) will generate one more electrostatic potential, as shown in Fig. 4(c). This profile is certainly unstable, and it will result in interfacial charge reconstruction and concentrate the interfacial charge to the top interface (the 9th and 11th atomic layers) of the BTO, generating a profile of the electrostatic potential shown in Fig. 4(d).

Surely, the effect of the quantum mechanical kinetic energy should be considered to obtain the final electrostatic potential profile. This consideration seems more complex and the kinetic energy makes the interfacial charges more dispersed. Due to these effects, the occupied electrons in the Ti ions have spin splitting and there are non-zero magnetic moments in these two atomic layers. The ferromagnetism of the $n=4$ superlattice is also the combinatory outcome of quantum kinetic effect, polar interface, and FE polarization.

In a general sense, for the ultra-thin YTO/BTO superlattices, the electronic structures can be quantitatively different

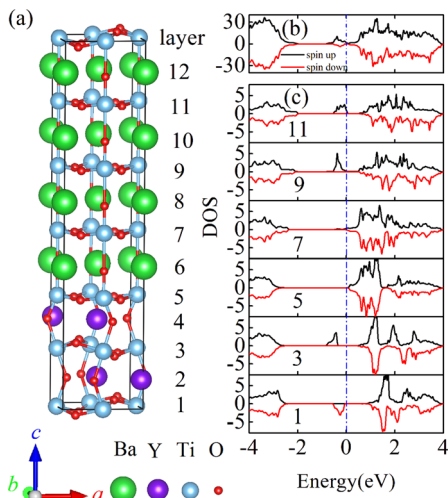


FIG. 3. (a) Schematic crystal structure of $(YTO)_2/(BTO)_4$. (b) Calculated spin-resolved total DOS, and (c) calculated PDOS of $(YTO)_2/(BTO)_4$. The Fermi energy is positioned as zero.

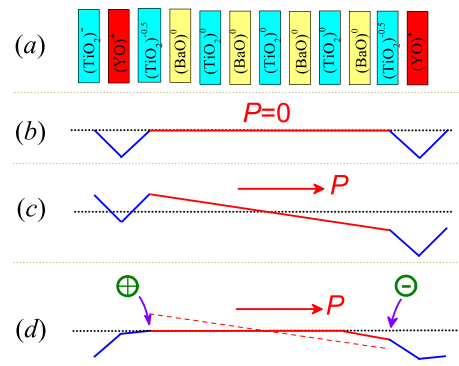


FIG. 4. (a) The atomic layers of the $n=4$ superlattice. (b) The electrostatic potential profile with no ferroelectric polarization ($P=0$). (c) The electrostatic potential profile with nonzero polarization, which evolves into the final profile in (d) upon considering the interfacial charge reconstruction. Here, no contribution from the quantum mechanical kinetic energy effect is considered yet.

for different combinations. For instance, when n is much bigger ($n > 10$), the Ti ions in the middle atomic layers of the BTO would be different from those near the interfaces. While the ferromagnetism across the BTO shows some inhomogeneity, the YTO/BTO interfacial 2DEG remains active. Due to the smooth progress in high quality layer-by-layer growth technique, such thin superlattices become accessible experimentally and thus the present work adds a promise to extensive exploration of ultra-thin oxide heterostructures and superlattices.

This work was supported by the National 973 Projects of China (Grant No. 2011CB922101), the Natural Science Foundation of China (Grant Nos. 11234005, 11274060, 51332006, and 51322206), and the Nantong University Natural Science Foundation (Grant No. 10Z003), China.

- ¹A. Ohtomo and H. Y. Hwang, *Nature (London)* **427**, 423 (2004).
- ²N. Reyren *et al.*, *Science* **317**, 1196 (2007).
- ³B. R. K. Nanda and S. Satpathy, *Phys. Rev. Lett.* **101**, 127201 (2008).
- ⁴Y. Wang *et al.*, *Phys. Rev. B* **79**, 212408 (2009).
- ⁵K. Rogdakis *et al.*, *Nat. Commun.* **3**, 1064 (2012).
- ⁶R. Pentcheva and W. E. Pickett, *Phys. Rev. Lett.* **99**, 016802 (2007).
- ⁷A. Brinkman *et al.*, *Nature Mater.* **6**, 493 (2007).
- ⁸Q. F. Zhang *et al.*, *Phys. Rev. B* **86**, 094403 (2012).
- ⁹R. Pentcheva and W. E. Pickett, *Phys. Rev. Lett.* **102**, 107602 (2009).
- ¹⁰M. Stengel, *Phys. Rev. Lett.* **106**, 136803 (2011).
- ¹¹M. Stengel *et al.*, *Phys. Rev. B* **83**, 235112 (2011).
- ¹²M. Stengel *et al.*, *Nature Mater.* **8**, 392 (2009).
- ¹³S. Okamoto *et al.*, *Phys. Rev. Lett.* **97**, 056802 (2006).
- ¹⁴P. Moetakef *et al.*, *Appl. Phys. Lett.* **99**, 232116 (2011).
- ¹⁵P. Moetakef *et al.*, *Phys. Rev. X* **2**, 021014 (2012).
- ¹⁶H. D. Zhou and J. B. Goodenough, *J. Phys.: Condens. Matter* **17**, 7395 (2005).
- ¹⁷P. Moetakef *et al.*, *Appl. Phys. Lett.* **98**, 112110 (2011).
- ¹⁸M. Mochizuki and M. Imada, *Phys. Rev. Lett.* **91**, 167203 (2003).
- ¹⁹A. C. Komarek *et al.*, *Phys. Rev. B* **75**, 224402 (2007).
- ²⁰M. Cwik *et al.*, *Phys. Rev. B* **68**, 060401 (2003).
- ²¹B. Keimer *et al.*, *Phys. Rev. Lett.* **85**, 3946 (2000).
- ²²X. Huang, Y. Tang, and S. Dong, *J. Appl. Phys.* **113**, 17E108 (2013).
- ²³G. Kresse and J. Hafner, *Phys. Rev. B* **47**, 558 (1993).
- ²⁴G. Kresse and J. Furthmüller, *Phys. Rev. B* **54**, 11169 (1996).
- ²⁵J. P. Perdew *et al.*, *Phys. Rev. Lett.* **77**, 3865 (1996).
- ²⁶S. L. Dudarev *et al.*, *Phys. Rev. B* **57**, 1505 (1998).
- ²⁷H. Sawada and K. Terakura, *Phys. Rev. B* **58**, 6831 (1998).
- ²⁸J. D. Garrett *et al.*, *Mater. Res. Bull.* **16**, 145 (1981).
- ²⁹Y. Okimoto *et al.*, *Phys. Rev. B* **51**, 9581 (1995).